

Changing the mindset in seismic data acquisition

A.J. "Guus" BERKHOUT, Delft University of Technology, the Netherlands

Seismic acquisition surveys are designed such that the time intervals between shots are sufficiently large to avoid the tail of the previous source response interfering with the next one (zero overlap in time). To economize on survey time and processing effort, the current compromise is to keep the number of shots to some acceptable minimum. The result is that in current practice the source domain is poorly sampled.

It is proposed to abandon the condition of nonoverlapping shot records. Instead, a plea is made to move to densely sampled and wide-azimuth source distributions with relatively small time intervals between consecutive shots ("blended acquisition"). The underlying rationale is that interpolating missing shot records, meaning generating data that have not been recorded, is much harder than separating the data of overlapping shot records. In other words, removing interference is preferred to removing aliasing.

A theoretical framework is presented that enables the design of blended 3D seismic surveys. This framework also provides directions about how to process blended data. The concept of blending has significant implications for both quality and economics.

Background

In land seismics, the concept of interfering shot records is known from vibroseis acquisition. The duration of a vibroseis survey is largely determined by the long signal sweeps of the vibroseis source (typically 10–20 s). These long sweeps are required to obtain the necessary signal-to-noise ratio. It makes vibroseis surveys time-consuming. To reduce survey time, methods have been developed to deploy various vibroseis groups simultaneously. These methods are based on transmitting specially encoded source sweeps. Codes have been designed such that the interfering source responses can be separated in a preprocessing step. The simultaneous vibroseis recording methods are known as slip-sweep, flip-flop, orthogonal sweeps, phase rotation, cascading, upsweep-downsweep, etc. Many oil companies and seismic contractors have their own patented methods. An overview of the various simultaneous vibroseis sweep methods is given by Bagaini (2006).

Beasley et al. (1998) propose to fire impulsive seismic sources at different locations at the same time ("simultaneous source firing"). They illustrate this concept with two sources off the ends of a marine cable and show with a 2D field example that CMP processing already provides a good separation between the overlapping source responses. Stefani et al. (2007) elaborate on this concept and introduce small random time delays as well ("near simultaneous source firing"). They demonstrate on 3D field data that the interference between the overlapping shot records of two spatially well-separated sources can be effectively suppressed by PSTM. Ikelle (2007)

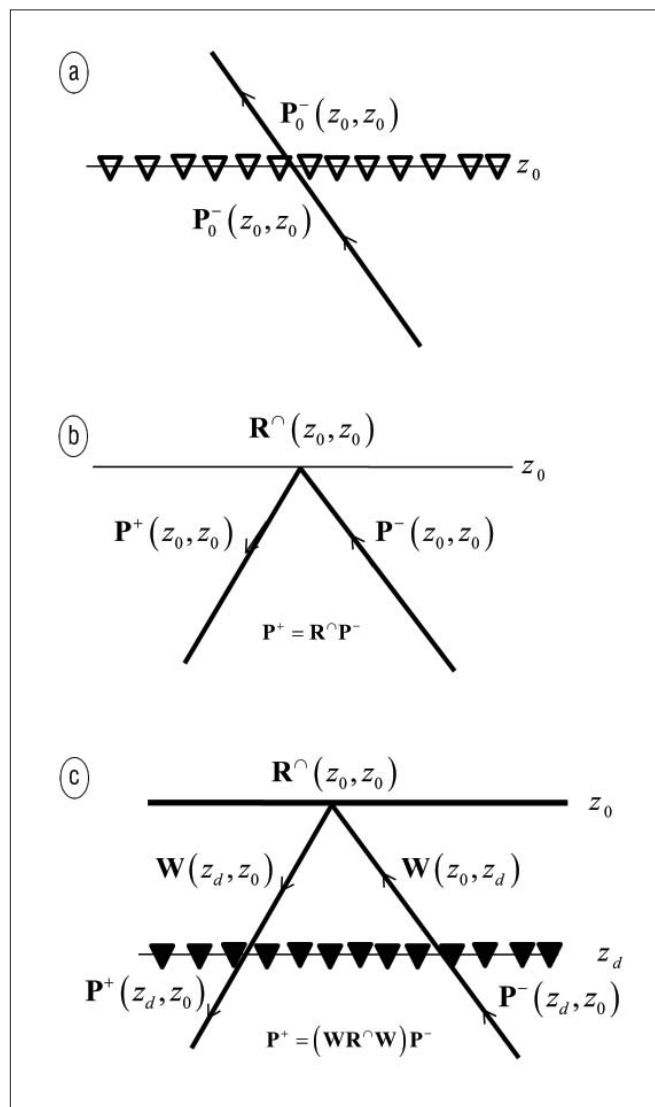


Figure 1. Up- and downgoing waves at and near the surface. Detector matrix $\mathbf{D}(z_d, z_0)$ contains both the properties of the detector arrays at z_d and the influence of the stress-free surface at z_0 . Wavefield operators \mathbf{W} represent propagation between z_d and z_0 ; wavefield operator \mathbf{R}^\wedge represents reflection at the lower side of z_0 . For a flat and stress-free surface $\mathbf{R}^\wedge = -\mathbf{I}$, where \mathbf{I} equals the unity matrix.

discusses the coding and decoding of seismic data using simultaneous sources on land or at sea. He shows that the response of four simultaneous shots, being fired four times with different amplitudes, defines a fully determined system that can be decomposed into the responses of the individual shots. To overcome being underdetermined, Ikelle suggests the use of higher-order statistics, sparseness constraints and prior knowledge.

In this paper, the method of (near) simultaneous shooting is extended to the system concept of blended acquisition, where blended acquisition stands for continuous recording

of multisource responses that overlap in time. The multisource properties are characterized by the combination of offsets, azimuths, and delay times. Encoded source signatures are not required and delay times may be large (up to seconds). The use of relatively large delay times makes blended acquisition different from (near) simultaneous shooting. It brings interference under user control. Note that for very large delay times, say larger than 20 s, blended acquisition equals traditional acquisition (no interference). A theoretical framework is proposed that enables the design of blended seismic acquisition with a focus on quality and economics. In addition, the proposed framework allows the formulation of a forward model for blended 3D seismic data. This model is used to propose different options for preprocessing blended data sets.

Operator presentation of seismic data

The large amount of discrete measurements of a seismic survey can be conveniently arranged with the aid of the so-called data matrix, \mathbf{P} , each column representing a shot record and each row representing a receiver gather. Hence, matrix element \mathbf{P}_{ij} represents a single trace that is related to source position j and detector position i . In the temporal frequency domain \mathbf{P}_{ij} is a complex-valued scalar, representing one frequency component of a seismic trace. Data matrix \mathbf{P} can be directly used for the formulation of wave-theory-based numerical algorithms in seismic processing such as multiple removal and prestack migration. After removal of the waves that have travelled along the surface, the data matrix can be expressed in terms of propagation and reflection operators (feedback model).

If matrix $\mathbf{X}_0(z_\rho, z_0)$ represents the multidimensional transfer function of the subsurface ($z > z_0$), then each element of $\mathbf{X}_0(z_\rho, z_0)$ contains the impulse response that was generated by a unit dipole source at z_0 and that was detected by a unit sensor at z_ρ . The subscript "0" in \mathbf{X}_0 indicates that the surface is a reflection-free boundary, meaning that the seismic signal has made only one round-trip through the subsurface (from z_0 to z_ρ). Using $\mathbf{X}_0(z_\rho, z_0)$ as a multidimensional wavefield operator, the measurements at reflection-free acquisition surface z_ρ , $\mathbf{P}_0(z_\rho, z_0)$, can be written as (Figure 1a):

$$\begin{aligned} \mathbf{P}_0(z_\rho, z_0) &= \mathbf{D}(z_\rho) \mathbf{P}_0^-(z_0, z_0) \\ &= \mathbf{D}(z_\rho) \mathbf{X}_0(z_\rho, z_0) \mathbf{S}^+(z_0), \end{aligned} \quad (1a)$$

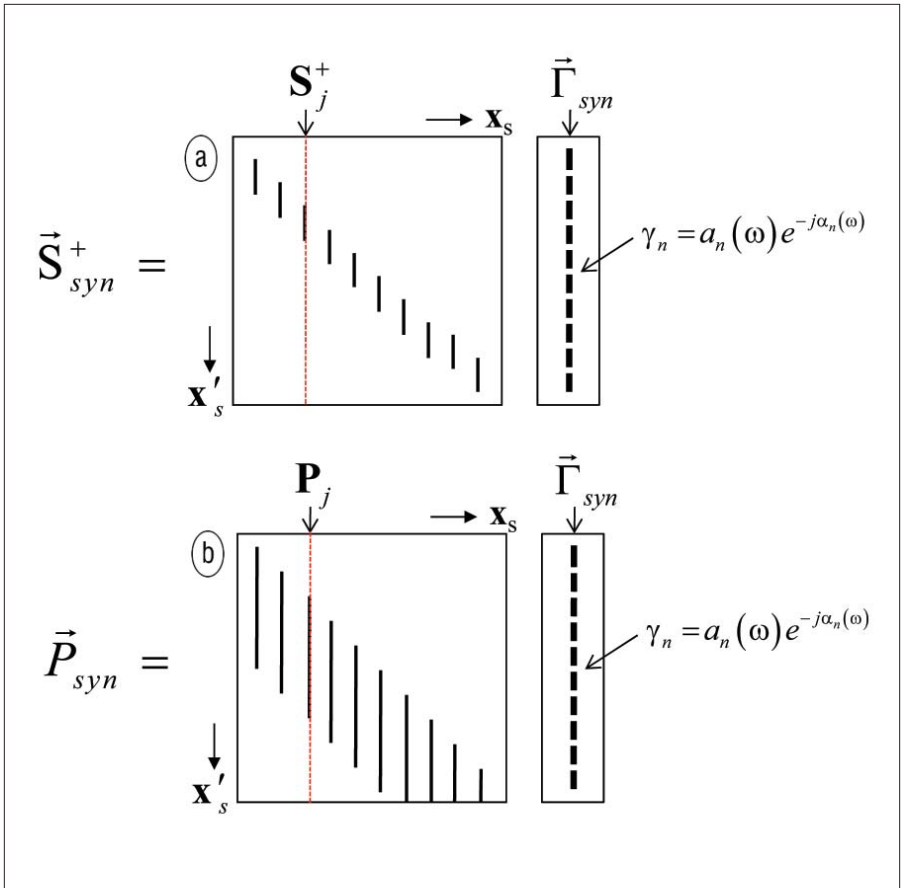


Figure 2. (a) Vector-matrix equation for synthesizing an areal source. From the physics point of view, this equation quantifies a weighted addition of the single sources as used in the field. (b) Vector matrix equation for synthesizing an areal source response. From the physics point of view, this equation quantifies a weighted addition of the shot records as measured in the field.

where $\mathbf{P}_0^-(z_\rho, z_0)$ is the upward travelling wavefield at z_0 . In Equation 1a, each column of source matrix \mathbf{S}^+ represents one source array as used in the field and, similarly, each row of detector matrix \mathbf{D} represents one detector array that transforms the upgoing wavefield (\mathbf{P}_0^-) into one measurement (one element of matrix \mathbf{P}_0). For a stress-free surface, both up- and downgoing wavefields exist (Figure 1b), and Equation 1a need be extended to:

$$\begin{aligned} \mathbf{P}(z_d, z_0) &= \mathbf{D}(z_d, z_0) \mathbf{P}^-(z_0, z_0) \\ &= \mathbf{D}(z_d, z_0) \mathbf{X}(z_0, z_0) \mathbf{S}^+(z_0), \end{aligned} \quad (1b)$$

where detector level z_d is generally closely situated at the surface (z_0) and transfer function $\mathbf{X}(z_\rho, z_0)$ includes the surface multiples. Unlike \mathbf{X}_0 , quantifying one seismic round-trip, \mathbf{X} quantifies many round-trips. In Equation 1b, matrix $\mathbf{D}(z_\rho, z_0)$ includes generation of the near-field surface ghost (Figure 1c). Note that Equations 1a and 1b represent the reflection data without and with surface multiples, respectively. Hence, by transforming the stress-free surface into a reflection-free surface, both the surface ghost and the surface multiples are removed from the data: from $\mathbf{P}(z_d, z_0)$ to $\mathbf{P}_0(z_\rho, z_0)$.

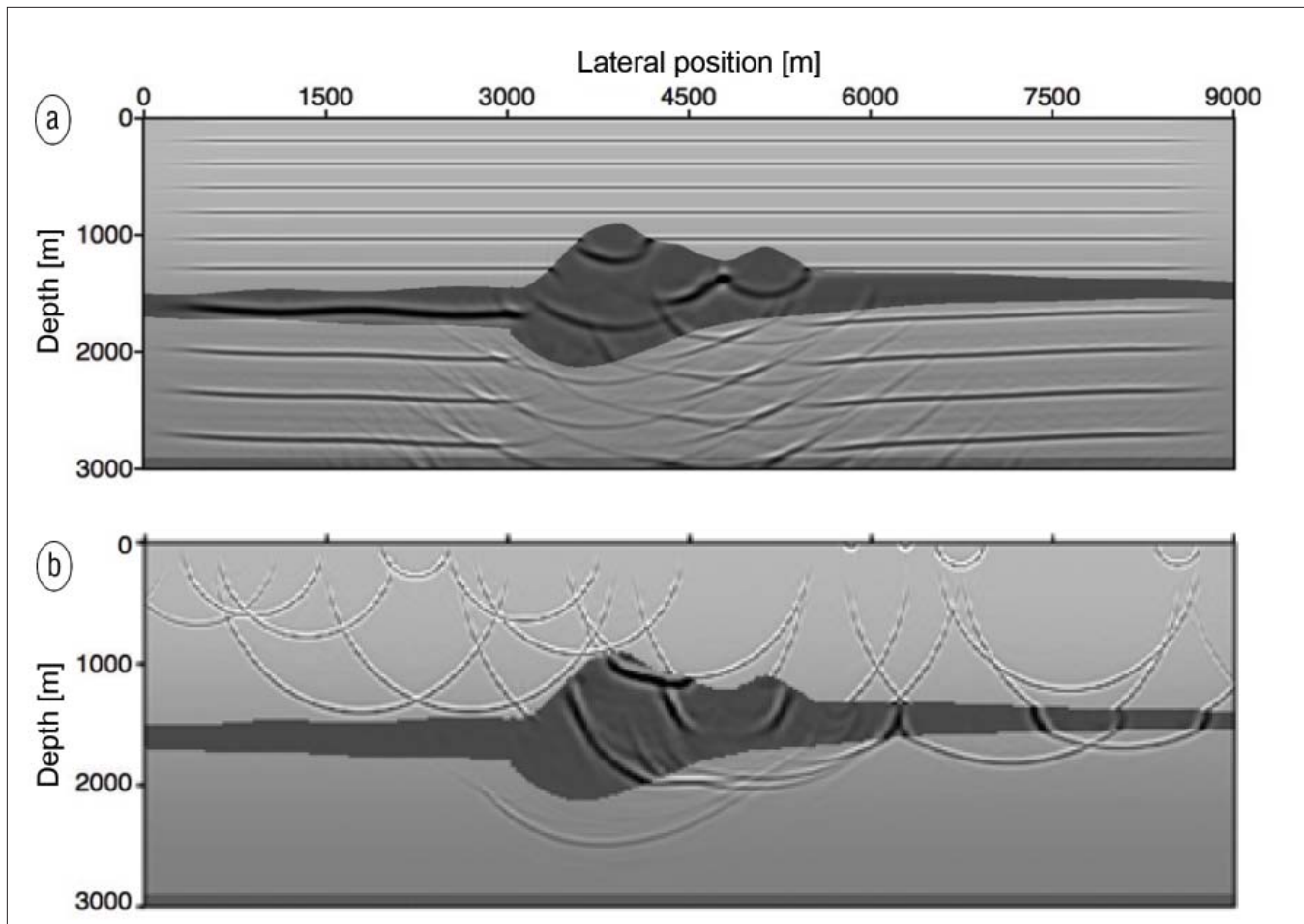


Figure 3. (a) Synthesis of a plane source wavefield according to Equation 2a, showing a number of snapshots. Synthesis yields a coherent source wavefield. (b) Simulation of a blended source wave field, according to Equation 3a, showing one snapshot. Blending yields an incoherent source wavefield.

Synthesis of areal shot records

Berkhout (1992) introduced the concept of areal shot records. Unlike a *conventional* shot record, being basically a point source response, an *areal* shot record is the response of a source with significant areal extension. This areal source may generate a downgoing source wavefield with any desired spatial shape. In the same publication, the synthesis operator Γ was introduced and examples were given for plane-wave sources, not only at the surface (z_0) but also at the target level (z_m), and focal sources with their focal points anywhere in the subsurface. Focal wavefields became the fundamental basis of the Common Focus Point (CFP) method.

If we define the synthesis operator by the column vector $\vec{\Gamma}_{syn}(z_0) = [\gamma_1, \gamma_2, \dots, \gamma_N]^T$, then any areal source can be written as a linear combination of point sources (Figure 2a):

$$\vec{S}_{syn}^+(z_0) = \mathbf{S}^+(z_0) \vec{\Gamma}_{syn}(z_0), \tag{2a}$$

where the synthesis coefficients, $\gamma_n = a_n(\omega) e^{-j\alpha_n(\omega)}$, determine the shape of the areal source wavefield. Using Equation 1b, the response of this areal source is given by the data vector (Figure 2b):

$$\vec{P}_{syn}(z_d, z_0) = \mathbf{P}(z_d, z_0) \vec{\Gamma}_{syn}(z_0). \tag{2b}$$

Equation 2b shows that the response of any areal source can be constructed by a weighted addition of the shot records as measured in the field.

Note that in the simple situation of synthesizing a plane wave source at the surface the elements of $\vec{\Gamma}_{syn}(z_0)$ are given by $\gamma_n = e^{-j\omega p x_n}$, p being the ray parameter of the plane wave. Figure 3a illustrates this for a horizontal plane wave. As early as the mid-1970s, Taner (1976) reported interesting results on plane wave synthesis at the surface. And in the mid-1980s, Rietveld (1985) showed how to generate plane waves at the reservoir level. Practical application, however, was (and still is) seriously hampered by the coarse sampling of the source space. In the following, the concept of wavefield synthesis is used to introduce the concept of “blended acquisition.”

Principle of blended seismic acquisition

Let us introduce the concept of *blending* in the source domain:

$$\vec{S}_{bl}^+(z_0) = \mathbf{S}^+(z_0) \vec{\Gamma}_{bl}(z_0), \tag{3a}$$

where column vector $\vec{\Gamma}_{bl}(z_0)$ is the blending operator:

$$\vec{\Gamma}_{bl}(z_0) = [\gamma_1, \gamma_2, \dots, \gamma_N]^T \tag{3b}$$

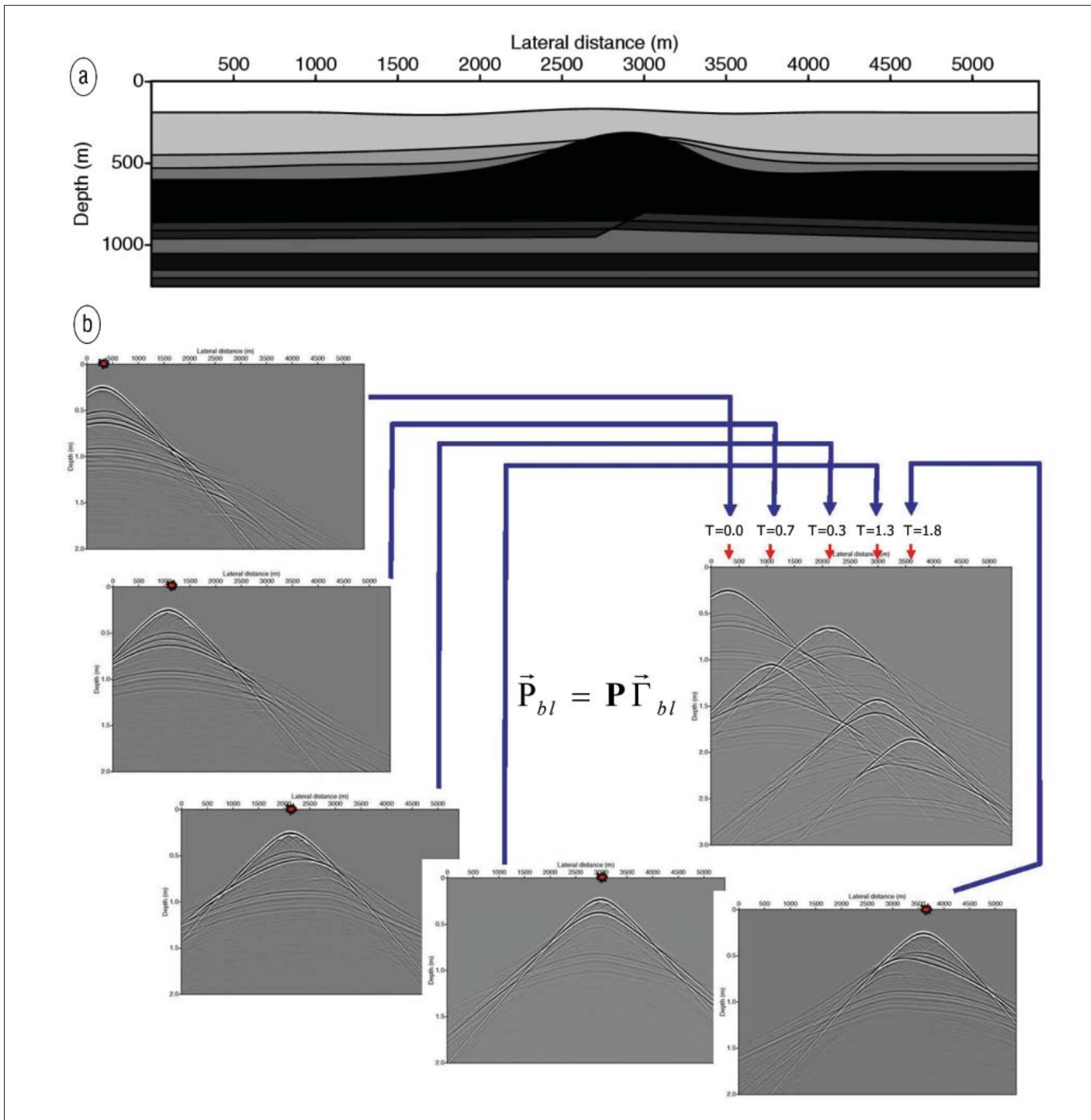


Figure 4. (a) Subsurface model that is used to simulate unblended and blended seismic data. (b) Simulation of one blended shot record according to Equation 4. In this illustration, the blended source configuration consists of five individual shots.

with $\gamma_n = e^{-j\omega T_n}$.

By comparing Equations 2a and 3a, we see that synthesis and blending both involve a linear combination of single sources. However, the fundamental difference between blending and synthesis is that in the synthesis process, the combined sources generate a continuous wavefront (plane, converging, diverging, etc.), while in blending a configuration of single sources generates separate wave fronts. Of course, these wavefronts interfere with each other (Figure 3b), but they do not merge into one wavefront (compare Figure 3b with Figure 3a). Blending is a process that creates incoherent

wavefields.

After combining Equations 1b and 3a, the blended seismic data are given by the data vector

$$\vec{P}_{bl}(z_d, z_0) = \mathbf{P}(z_d, z_0) \vec{\Gamma}_{bl}(z_0). \quad (4)$$

Equation 4 shows that blended seismic data can be simulated from densely sampled, unblended field records by weighted addition.

Figure 4 shows the principle. For the subsurface model in Figure 4a, unblended field records were simulated with source

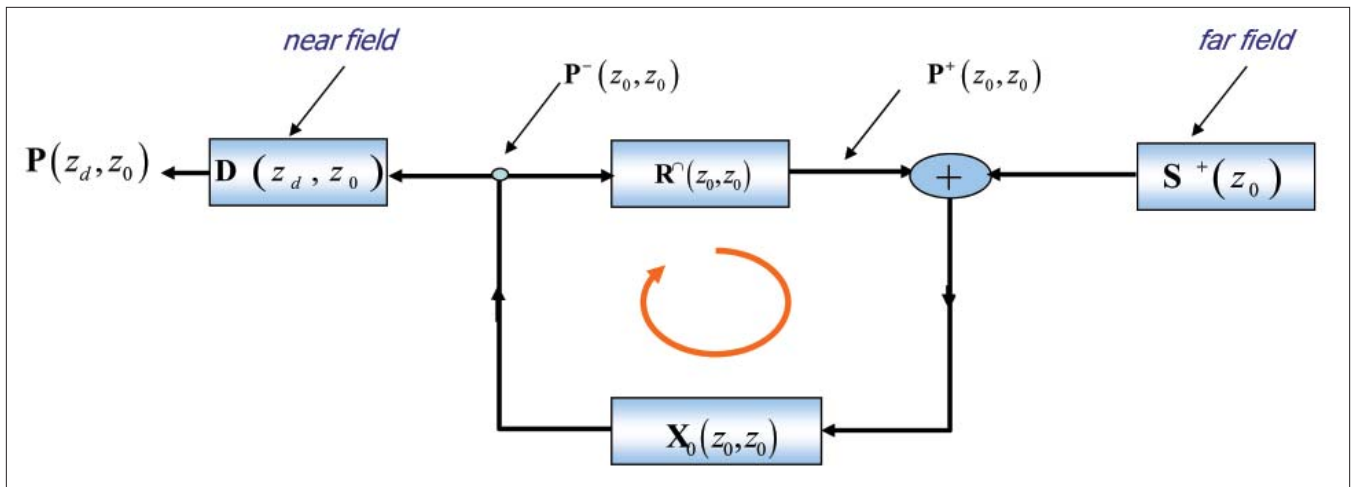


Figure 5. Feedback model, showing the generation of primary reflections (one round-trip) and surface-related multiple scattering (many round-trips). Each wavefield operator is presented by a matrix

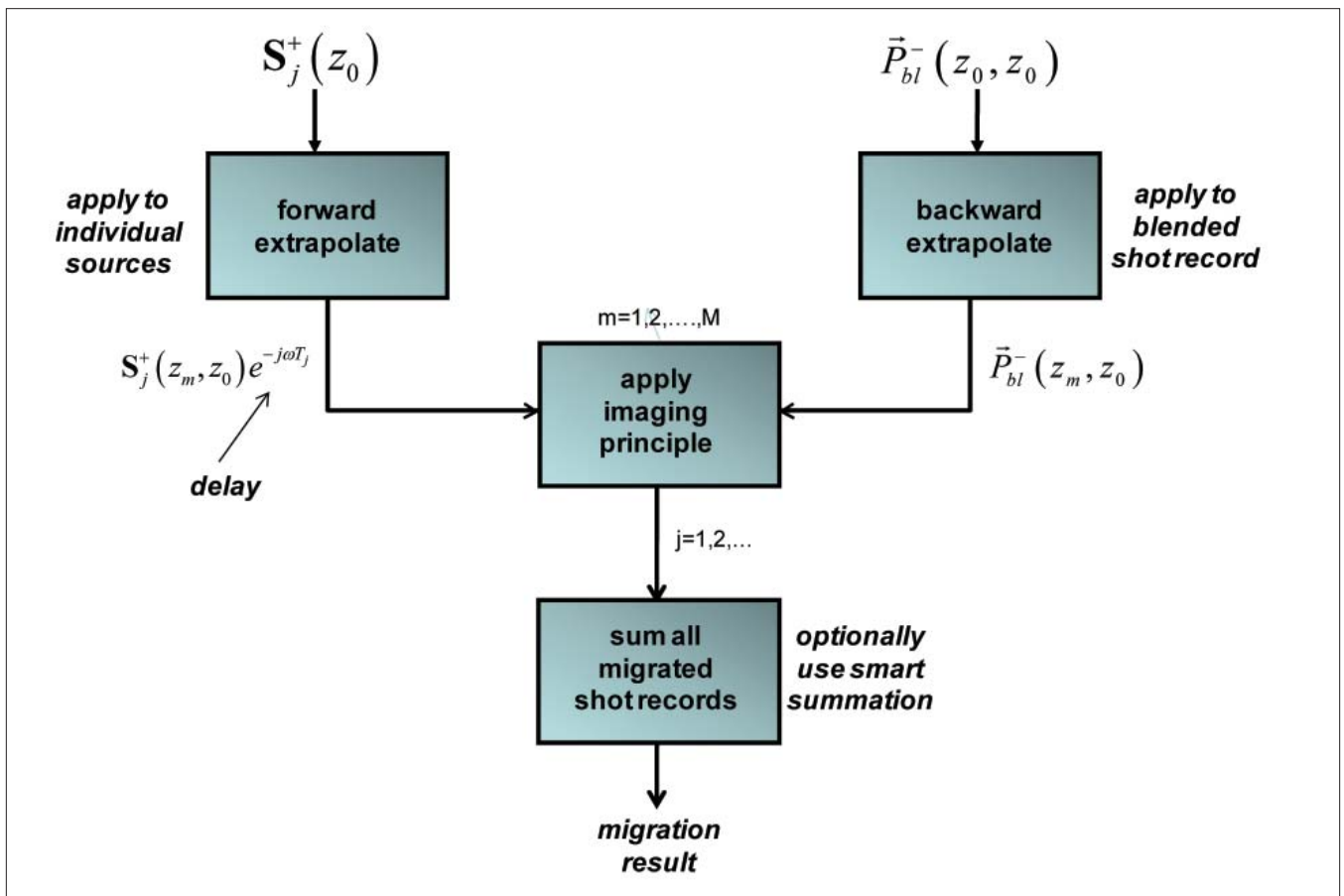


Figure 6. Migration scheme for a blended shot record (no pre-deblending). Note that all involved sources of the blended shot record are individually extrapolated, but the blended shot record is extrapolated only once. This means that one blended shot record yields SDR-migrated shot records.

spacing $\delta x_s = 60$ m, and a blending process was carried out according to Equation 4. For this illustration, five field records were blended with source emission times (in seconds): $T_1 = 0.0$, $T_2 = 0.7$, $T_3 = 0.3$, $T_4 = 1.3$, $T_5 = 1.8$. This is visualized in Figure 4b. In practice, one blended shot record may involve many more sources. This choice is part of acquisition design. Note that, unlike the multiple problem, interference due to blending is fully under user control (choice of T_n).

A key performance indicator in the design of blended seismic surveys is the source density ratio:

$$SDR = \frac{\text{number of sources in the blended survey}}{\text{number of sources in the unblended survey}}$$

In the 2D example of Figure 4, the $SDR=5$, but in 3D it could be (and should be) significantly higher.

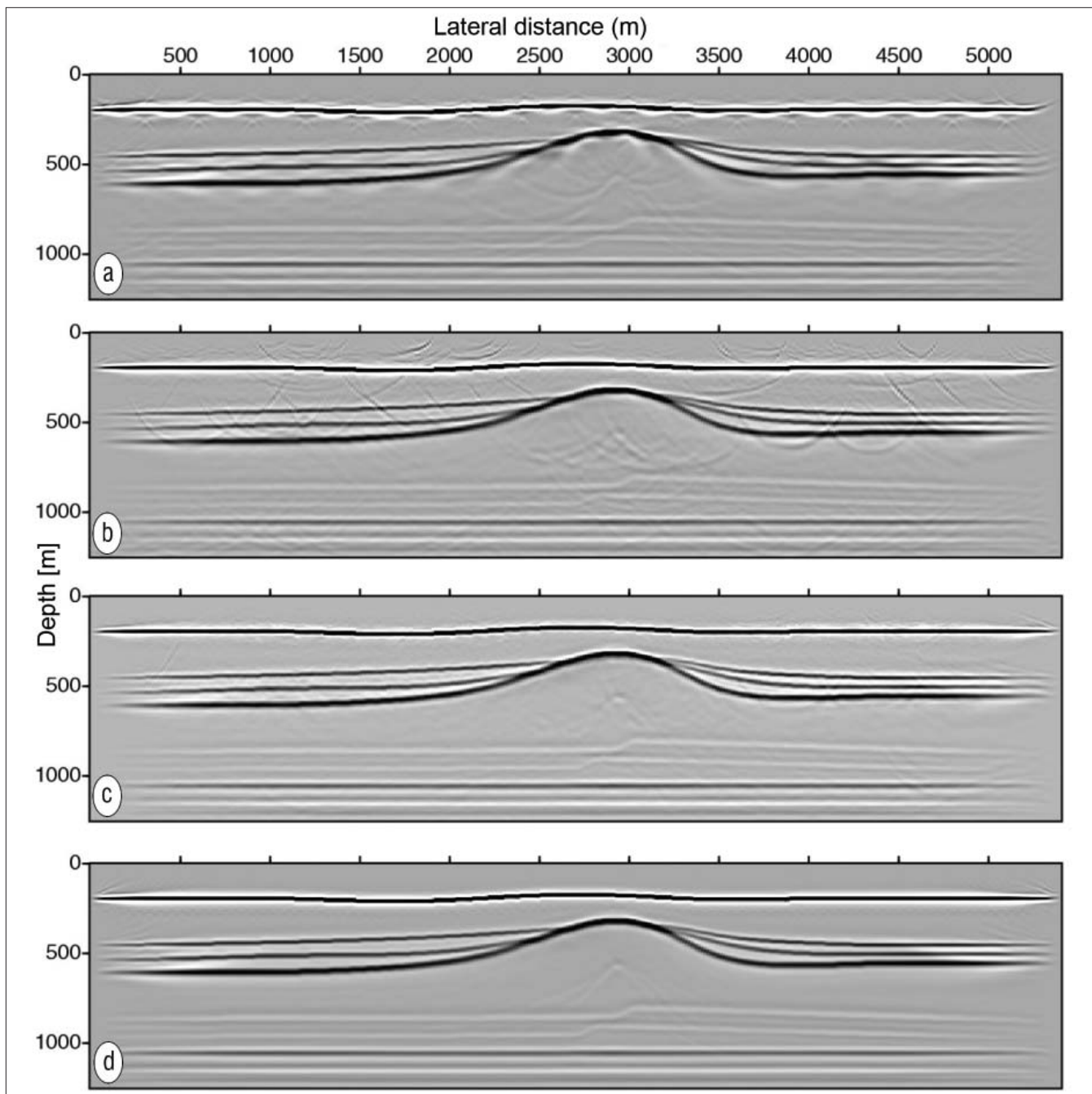


Figure 7. (a) Migration of unblended shot records ($\Delta x_s = 300$ m). (b) Migration of blended shot records ($SDR = 5$) according to the scheme in Figure 6. (c) Migration of blended shot records ($SDR = 5$) according to the scheme in Figure 6, using median stacking when adding the migrated shot records. (d) Migration of unblended shot records after perfect deblending ($\delta X_s = 60$ m).

Forward model of unblended seismic data

Figure 5 shows schematically the up- and downgoing wavefields as they occur at the stress-free surface (z_0). Using the operator presentation in Figure 5, leaving (z_0, z_0) out of the notation, it can be easily verified that these wavefields can be written as

$$\begin{aligned}
 \mathbf{P}^- &= \mathbf{X}_0 \mathbf{S}^+ + \mathbf{X}_0 \mathbf{P}^+ \\
 &= \text{primaries} + \text{multiples},
 \end{aligned}
 \tag{5a}$$

where the up- and downgoing waves, \mathbf{P}^+ and \mathbf{P}^- , are interrelated by the surface reflection coefficient:

$$\mathbf{P}^+ = \mathbf{R}^{\cap} \mathbf{P}^-, \tag{5b}$$

superscript “ \cap ” indicating that reflection occurs at the lower side of the surface. In Equation 5a, the primaries have traveled one round-trip and the multiples have traveled many round-trips. Note that primaries are used here in a wider sense, including internal multiples as well.

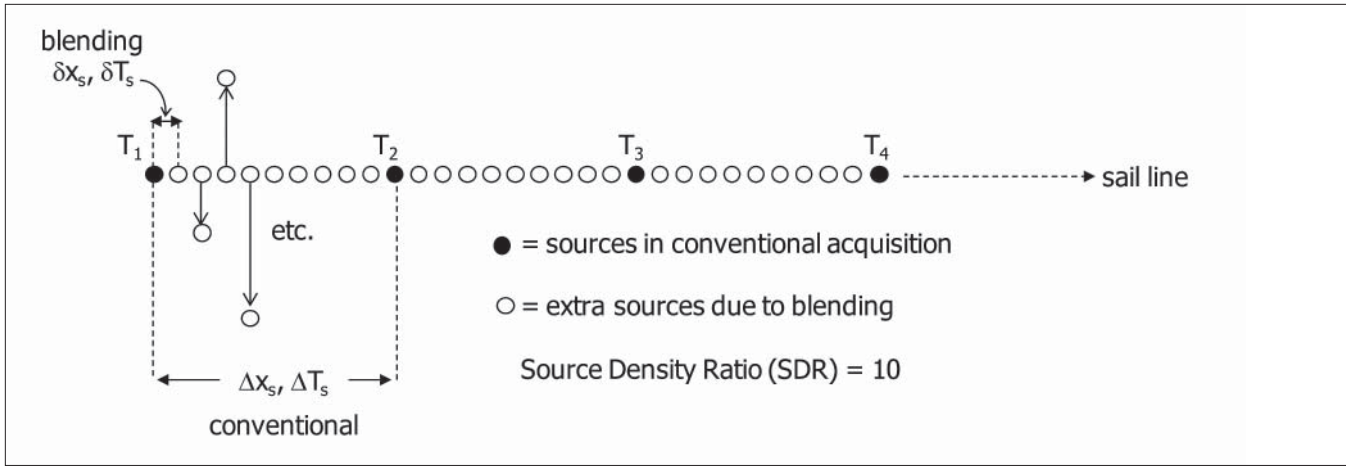


Figure 8. Spatial and temporal source properties of conventional acquisition as well as blended acquisition. Note that blending allows for a large increase of the source density as well as an improved azimuth distribution.

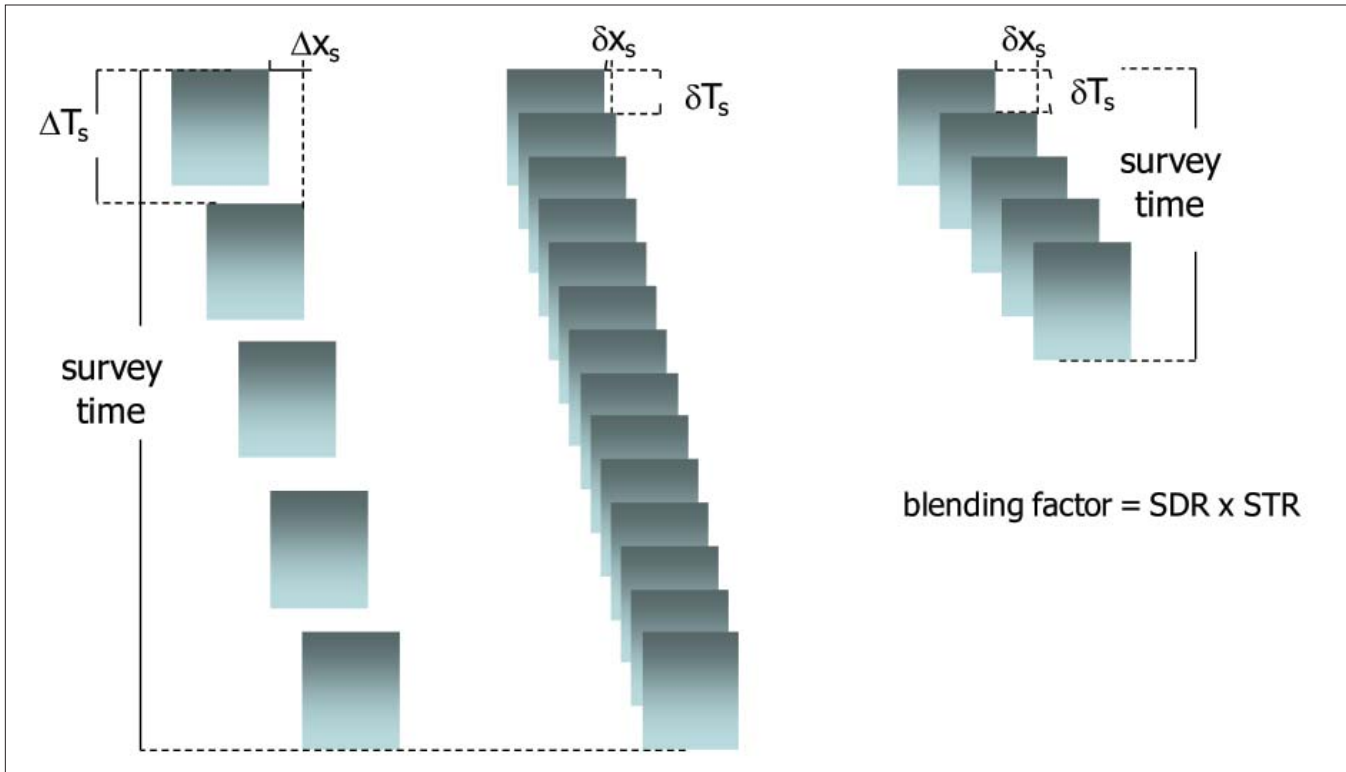


Figure 9. (left) Conventional seismic acquisition without blending. (center) Blending with focus on quality: by reducing the source interval times while keeping the survey time unchanged, the number of shots can be significantly increased. (right) Blending with focus on survey time: by decreasing the source interval times while keeping the number of shots unchanged, the survey time can be significantly reduced. Of course, any mixture may be chosen.

Forward model of blended seismic data

Using Equation 5a, simulation of the blending process can be formulated as:

$$\mathbf{P}^- \bar{\Gamma}_{bl} = \mathbf{X}_0 \mathbf{S}^+ \bar{\Gamma}_{bl} + \mathbf{X}_0 \mathbf{P}^+ \bar{\Gamma}_{bl} \tag{6}$$

= blended primaries + blended multiples.

Hence, if we carry out blended acquisition in the field, then the model of a physically recorded blended shot record can be presented by the data vector:

$$\bar{P}_{bl}^- = \mathbf{X}_0 \bar{S}_{bl}^+ + \mathbf{X}_0 \bar{P}_{bl}^+, \tag{7a}$$

where the blended up- and downgoing waves, \bar{P}_{bl}^- and \bar{P}_{bl}^+ , are interrelated by the surface reflection coefficient:

$$\bar{P}_{bl}^+ = \mathbf{R} \bar{P}_{bl}^-. \tag{7b}$$

In Equation 7a, the blended primaries have traveled one round-trip and the blended multiples have traveled many round-trips.

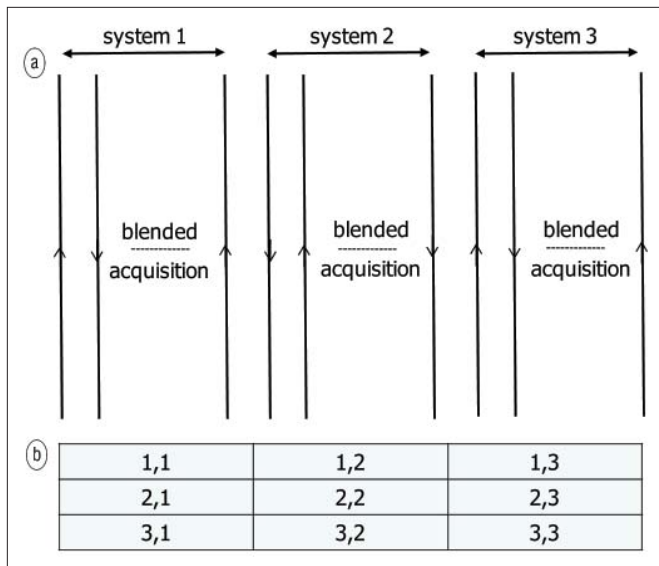


Figure 10. The concept of crossblended seismic acquisition. In this example, crossblending is shown, leading to a decrease of the total survey time by a factor of three ($STR = 3$). Using five shots in one blended source, an increase of information is achieved by a factor of 45 ($SDR = 45$). Together, it results in a blending factor of 135. Note that each acquisition system may use its own blending operator.

If Equation 7b is substituted into Equation 7a, then the blended version of the well-known multiple scattering equation is obtained:

$$\bar{P}_{bl}^- = \mathbf{X}_0 \bar{S}_{bl}^+ + \mathbf{X}_0 \mathbf{R} \bar{P}_{bl}^- \quad (8)$$

We will use Equation 8 later in this paper to show that surface multiples can be directly removed from blended data.

Exploring the impact of interference

To get a feeling for the effect of interference, an example of migrating blended data is given. The blended shot records used have been simulated via the blending process shown in Figure 4. Shot record migration was carried out by forward extrapolating the wavefield of each individual source, taking into account the source delay in the extrapolation process, followed by backward extrapolating the blended shot record. Figure 6 shows the migration scheme. Note that for this example one blended shot array consists of five sources and, therefore, the scheme yields five times as many migrated output records as blended input records ($SDR = 5$). Figure 7 compares the different migration results: unblended input versus blended input. Looking at the large interference effects in the blended shot records, we may conclude that the migration process suppresses these effects very well, particularly if the migrated shot records are added by median stacking. As expected, the image of the blended data has better resolution properties than the image of the conventional data ($SDR = 5$).

Intelligent blending, strategic considerations

The concept of blended acquisition creates extra degrees of freedom in the acquisition design: where do we position the

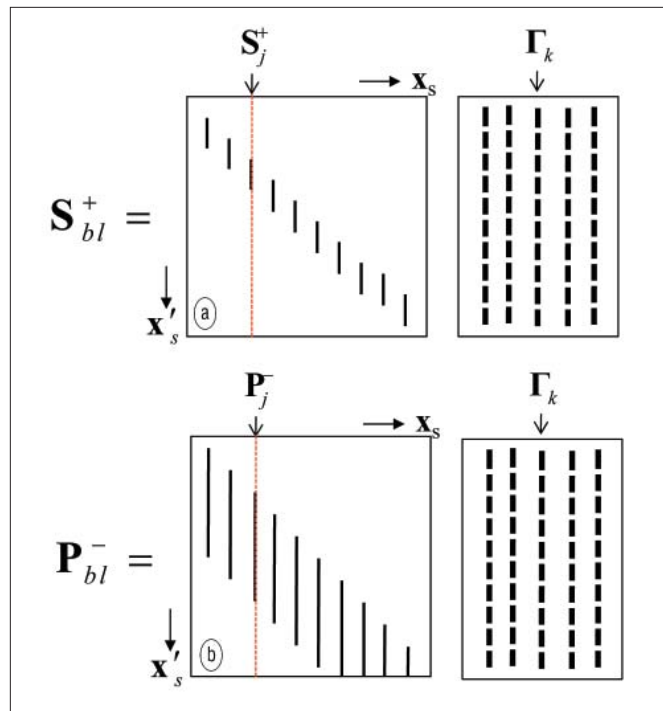


Figure 11. (a) One column of a blended source matrix represents a blended source array, and each element of a blended source array represents a single "point" source with a space-dependent time delay. (b) One column of a blended data matrix represents one blended shot record, and each element of a blended shot record represents a superposition of time-delayed traces.

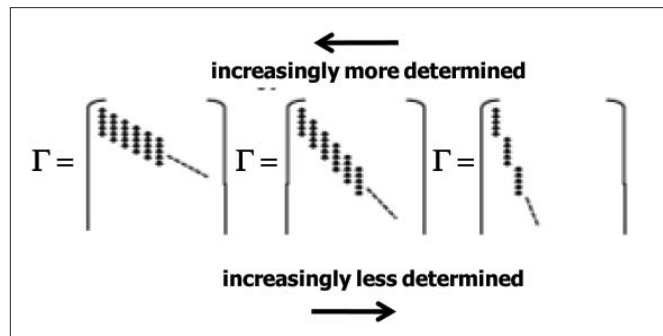


Figure 12. How well blended data can be deblended is controlled by the acquisition design: fully determined (left), underdetermined (middle), fully undetermined (right).

extra shots and how do we choose the delay times between those shots? More specific, in the blending concept, each coherent source (pattern) in the traditional survey is replaced by an incoherent source array in the blended survey (Figure 8). The blended source arrays can be characterized by three attributes: the number of sources (size of the array); the distribution of offsets and azimuths (spatial configuration of the array); and the distribution of delay times (temporal configuration of the array). This differs from the 1D concept of encoding the source signature. Actually, if one still would like to think in terms of source encoding, the proposal here is a 3D encoding, where the required change on the source signature is minimal, (i.e., just a time delay). This means that increased complexity on the seismic source is avoided,

or could be even decreased. The option to decrease source complexity in blended acquisition will be clarified later in this paper.

On the one hand, the focus of blended acquisition can be on image quality, with the benefit of a denser spatial sampling and a wider range of azimuths. For this reason we have already proposed the key performance indicator SDR. On the other hand, the focus can also be put on *survey time* (i.e., blended acquisition is carried out with the same number of shots), but with reduced survey time. Figures 9a and 9b illustrate that a higher source density leads to a reduced spatial source interval for the same survey time. In Figure 9b the focus is on quality: a denser spatial source sampling means better illumination of the subsurface. Figures 9a and 9c illustrate that the survey time can be decreased while the number of shots stays the same. This option may be particularly valuable in the situation of multioffset/multi-azimuth VSP acquisition, saving very costly borehole time. To emphasize this economic aspect of blended acquisition, a second key performance indicator is proposed that quantifies the gain in acquisition time (survey time ratio):

$$STR = \frac{\text{number of acquisition days in the unblended survey}}{\text{number of acquisition days in the blended survey}}$$

In many practical situations, it is essential that seismic surveys are carried out in a small time window (“acquisition slot”). Think at the limited accessibility of permafrost areas, bad weather regions, biologically protected environments, borehole availability in VSP, high repetition rates in seismic production monitoring, etc. Blended acquisition with an $STR > 1$ will create a new opportunity in these cases. For instance, instead of working with one traditional marine acquisition system—the combination of source boat with cable vessel—one could use several blended acquisition systems at the same time (concept of crossblending). Figure 10 shows the parallel utilization of three blended systems. This smart design does not only lead to a decrease of survey time by a factor of three ($STR = 3$), when using five sources for one blended shot record, it also increases the source density by a factor of 45 ($SDR = 3^2 \times 5$). The result is an increase of information by 45 in 1/3 of the time! To characterize the acquisition performance of blended surveys by one number, the blending factor is proposed: *blending factor* = *source density ratio* \times *survey time ratio*

For the above example, the blending factor equals 135. Note that if the tow speed of the recording vessel could be increased by a factor of two, then $STR = 6$. Note also that if the number of cables would be decreased by a factor of three, then the total amount of information is still increased by a factor of 15. It illustrates that many variations are possible to optimize both quality and economics.

Acquisition design

In multishot blended acquisition surveys, the source vector matrix is replaced by:

$$\mathbf{S}_{bl}^+ = \mathbf{S}^+ \mathbf{\Gamma}_{bl}, \quad (9)$$

each column of $\mathbf{\Gamma}_{bl}$ representing one blended source array and each column of matrix $\mathbf{\Gamma}_{bl}$ defining the 3D configuration (offsets, azimuths, delay times) of a blended source array (Figure 11a). Hence, a column of $\mathbf{\Gamma}_{bl}$ determines the illumination capabilities of a blended source array and, therefore, the information content of the related blended shot record.

It is proposed to design a blended acquisition survey such that, for a prespecified number of source boats/vibrator units,

$$\mathbf{\Gamma} \mathbf{\Gamma}^{-1} - \mathbf{I} = \text{minimum} \quad (10a)$$

or

$$\mathbf{\Gamma} \mathbf{\Lambda} \mathbf{\Gamma}^H - \mathbf{I} = \text{minimum}, \quad (10b)$$

\mathbf{I} being the unity matrix. In Equation 10b, $\mathbf{\Lambda} = (\mathbf{\Gamma}^H \mathbf{\Gamma})^{-1}$ in case an L_2 -norm is used, superscript H meaning that the transpose should be taken.

Design conditions 10a and 10b aim at

$$\mathbf{S}_{bl}^+ \mathbf{\Gamma}^{-1} - \mathbf{S}^+ = \text{minimum} \quad (11a)$$

or

$$\mathbf{S}_{bl}^+ \mathbf{\Lambda} \mathbf{\Gamma}^H - \mathbf{S}^+ = \text{minimum}. \quad (11b)$$

In physical terms, Equations 11a and 11b show that in the computer a blended source can be approximately decomposed into its unblended components: deblending. The better the design, the better the decomposition. In practice the number of blended records will be smaller than the number of unblended records. This means that the system is underdetermined. In Figure 12, $\mathbf{\Gamma}$ is shown for three cases of five blended sources: from fully determined (left) to underdetermined (middle) to fully undetermined (right). In the fully undetermined case, the deblending procedure relies on properties like causality and source sparseness, and data-driven considerations. Therefore, inversion of blending operator $\mathbf{\Gamma}$ should be done in combination with processing algorithms.

For nearby sources, the difference in arrival times between overlapping shot records is largely given by the superposition of differential moveout and source delay time. Hence, the deeper the reflections, the more the differences in arrival time will approach the delay times that are given to the sources of the blended shot records. It is therefore advised to assign to nearby sources relatively large delay differences to avoid high correlation between unblended signal and interference noise: constrained minimization of Equations 11a and 11b. The correlation issue is very well known from the subtraction problem in multiple removal.

Deblending as a preprocessing step

In blended acquisition, the data matrix is given by

$$\mathbf{P}_{bl} = \mathbf{P} \mathbf{\Gamma}_{bl} \quad (12)$$

each column of \mathbf{P}_{bl} representing a blended shot record (Figure 11b). From Equation 12 it follows that the deblending

process in the forward data space can be formulated as

$$\mathbf{P} = \mathbf{P}_{bl} \Gamma^{-1} \quad (13a)$$

or

$$\mathbf{P} = \mathbf{P}_{bl} \Lambda \Gamma^H, \quad (13b)$$

Λ being determined by Equation 11b.

Equations 13a and 13b mean that all the interference effects in the measured blended shot records are approximately removed. The better the acquisition design, the better the approximation. Note that in the migration example (Figure 7), we actually approximated Γ^{-1} by Γ^H ("pseudo deblending"). This means that there is a lot of room for improvement!

Using Equation 12, it can be easily verified that blended data in the inverse data space can be formulated

$$\mathbf{P}_{bl}^{-1} = \Gamma_{bl}^{-1} \mathbf{P}^{-1} \quad (14a)$$

or

$$\mathbf{P}^{-1} = \Gamma_{bl} \mathbf{P}_{bl}^{-1}. \quad (14b)$$

This is an interesting result, as Equation 14b tells us that the unblended data in the inverse data space are obtained by a double forward blending process, once during acquisition and once during preprocessing.

Note that in the inverse data space all surface-related multiples map onto the origin (Berkhout, 2006):

$$\mathbf{P}^{-1} = \mathbf{P}_0^{-1} - \mathbf{A} \quad (15a)$$

with

$$\mathbf{A} = \mathbf{S}^{-1} \mathbf{R} \cap \mathbf{D}^{-1}. \quad (15b)$$

This means that, similar to deblending, multiple removal is simple in the inverse data space.

An outlook of processing blended data

It is self-evident that blended data are deblended first in a preprocessing step, followed by conventional processing such as multiple removal and migration. However, in the following we will outline that processing can also be directly applied to the blended measurements. This option has the significant advantage that model information can be included in the implicit deblending process, allowing data-driven optimization.

Combining deblending and multiple removal. Using the feedback model (Figure 5) and Equations 5a, and 5b, the measured data with surface-related multiples can be written as

$$\mathbf{P}^- = \mathbf{X}_0 \mathbf{S}^+ + \mathbf{X}_0 \mathbf{R} \cap \mathbf{P}^- \quad (16a)$$

or, including detector matrix \mathbf{D} ,

$$\mathbf{P} = \mathbf{P}_0 + \mathbf{P}_0 \mathbf{A} \mathbf{P} \quad (16b)$$

In Equation 16b, \mathbf{P}_0 , \mathbf{P} and \mathbf{A} are given by Equations 1a, 1b, and 15b, respectively.

The blended version of Equation 16b equals

$$\mathbf{P} \Gamma_{bl} = \mathbf{P}_0 \Gamma_{bl} + \mathbf{P}_0 \mathbf{A} \mathbf{P} \Gamma_{bl} \quad (17a)$$

or

$$\mathbf{P}_{bl} = \mathbf{P}_{0,bl} + \mathbf{P}_0 \mathbf{A} \mathbf{P}_{bl} \quad (17b)$$

or

$$\mathbf{P}_{bl} = \mathbf{P}_{0,bl} + \mathbf{P}_{0,bl} \mathbf{A}_{bl} \mathbf{P}_{bl} \quad (17c)$$

with

$$\mathbf{A}_{bl} = \Gamma_{bl}^{-1} \mathbf{A}. \quad (17d)$$

Equation 17c has exactly the same structure as Equation 16b and, therefore, surface multiples can be directly removed from the blended data with the iterative scheme for unblended data (see e.g., Verschuur and Berkhout, 1997). Following this iterative scheme, the first iteration starts with the initial estimates $\mathbf{P}_{0,bl} = \mathbf{P}_0 \Gamma_{bl}$ and $\Gamma_{bl} = \Gamma_{bl}^{-1} \mathbf{I}$. The final output consists of blended data without surface multiples:

$$\mathbf{P}_{0,bl} = \mathbf{P}_0 \Gamma_{bl} \quad (18a)$$

It is interesting to realize that in the iterative scheme Γ_{bl}^{-1} is optimized by implicitly using information in the surface multiples (data-driven optimization of the deblending process). This opens the opportunity to combine multiple removal with deblending:

$$\mathbf{X}_0 = \mathbf{P}_{0,bl} \mathbf{A}_{bl} \quad (18b)$$

Removal of blended multiples is currently under investigation.

Combining deblending with migration. In Figure 6, a migration scheme has been proposed for blended shot records (no deblending):

$$\mathbf{F} \mathbf{P}_{0,bl}^- - \mathbf{R} \mathbf{W} \mathbf{S}^+ = \text{minimum for each depth level} \quad (19a)$$

where \mathbf{R} represents the desired, deblended, angle-dependent reflectivity at a given depth level, \mathbf{W} equals the forward extrapolation operator, and \mathbf{F} equals the backward extrapolation operator to that depth level. Similarly, each column of $\mathbf{F} \mathbf{P}_{0,bl}^-$ represents the blended CFP-gather (without surface multiples) and each column of $\mathbf{W} \mathbf{S}^+$ represents the unblended incident source wavefield for that depth level. Equation 19a can be extended to properly handle all blended wavefields, reflected and incident, in the migration process:

$$\mathbf{F} \mathbf{P}_{bl}^- - \mathbf{R} \mathbf{W} \mathbf{S}_{bl}^+ - \mathbf{R} \mathbf{W} \mathbf{P}_{bl}^+ = \text{minimum for each depth level} \quad (19b)$$

where $\mathbf{F} \mathbf{P}_{bl}^-$ represents the blended CFP-gathers (with surface multiples), $\mathbf{W} \mathbf{S}_{bl}^+$ equals the blended incident source wavefields and $\mathbf{W} \mathbf{P}_{bl}^+$ equals the blended incident multiple wavefields. Note that estimation of \mathbf{R} occurs by making use of both the blended source wavefield and the blended surface multiples (double illumination). The author believes that Equation 19b describes the seismic imaging technology for the future.

Conclusions

It is proposed to replace current seismic acquisition methods (discontinuous recording, zero overlap in time) by a blended alternative (continuous recording, significant overlap in time). It is believed that the *interpolation* of missing shot records in conventional acquisition is much harder to accomplish than the separation of overlapping shot records in blended acquisition. The key input parameter in blending is the source delay time (T_n) for each individual source. For a given source configuration, T_n brings the interference in the blended recordings under user control.

With the focus on quality, blended acquisition allows significantly denser spatial source sampling and a much wider range of source azimuths. These properties may lead to the next principal step—improvement in seismic imaging quality. For instance, blended acquisition may improve the quality of seismic production monitoring significantly.

With the focus on economics, the blending concept allows significantly shorter survey times. This property will be particularly valuable in critical situations where small acquisition time windows dominate due to severe safety, environmental or economic restrictions. For instance, blended acquisition may improve the economics of VSP significantly. In crossblended acquisition, several acquisition systems are shooting and recording blended data at the same time. Crossblending allows better image quality as well as shorter survey times. For instance, in triple crossblending with five sources per blended shot record the survey time decreases with a factor of three (STR = 3) and the source density increases with a factor of 45 (SDR = 45). This leads to a blending factor of 135. High blending factors open new opportunities in situations where both image quality and survey time are critical.

A wave theoretical forward model for blended data is proposed. This model shows that the design of blended acquisition requires the optimization of a multidimensional blending operator. This operator is represented by a matrix and, therefore, deblending can be formulated in terms of matrix inversion (preprocessing step). In addition, nearby sources should have relatively large differential delay times.

An outlook for processing blended shot records is given. Two options are proposed. In option 1, a preprocessing step is described by applying a data driven inverse of the blending operator to the blended measurements (“deblending”). The result represents deblended data, with a relatively high source density, that can be used in standard seismic processing. In option 2, processing is directly applied to the blended data and it is shown how this could be done for surface multiple removal and prestack migration. Option 2 may be the start of a new learning process in seismic processing and seismic inversion.

Looking into the future, blended acquisition means rethinking current practice. New challenges are emerging by the requirements of high-quality continuous recording equipment, the availability of many more shooting boats/vibrator units and, for towed streamers, the implementation of high-speed cable vessels. Hence, the concept of blended acquisition

may initiate a range of new development activities to renovate current seismic acquisition systems: innovations build on innovations (Berkhout et al., 2007).

Using existing acquisition modules, the blended areal source consists of a configuration of equal seismic sources, such as air-gun arrays (marine) and vibroseis patterns (land). In the blending concept, however, the use of coherent field arrays can be abandoned and the assumption of equal sources is not required. Making the elements of the blending operator frequency-dependent,

$$\gamma_n = a_n(\omega)e^{-j\omega}, \quad (20)$$

sources with different properties can be included in the design. For instance, if we would use band-limited sources which together cover the total seismic bandwidth, then seismic sources may become significantly less complex and source density could be chosen in a frequency dependent manner (more high-frequency than low-frequency sources). Applying this concept, blended surveys may be carried out by acquisition systems that are a lot less complex and a lot more effective than the ones that are used today.

The measurements in passive seismics can be considered as blended data, the sources being of a natural nature (no user control on source locations and source delays). An interesting consequence of this view is that a unified theoretical framework can be derived for both passive and active seismic methods, resulting in a scientific model for natural and man-made blending. In addition, new insights can be gained in the possibilities and impossibilities of seismic interferometry.

Suggested reading. “Overview of simultaneous vibroseis acquisition methods” by Bagaini (SEG 2006 *Expanded Abstracts*). “A new look at simultaneous sources” by Beasley et al. (SEG 1998 *Expanded Abstracts*). “Areal shot record technology” by Berkhout (*Journal of Seismic Exploration*, 1992). “Prestack migration in terms of double focusing” by Berkhout, (*Journal of Seismic Exploration*, 1995). “Seismic processing in the inverse data space” by Berkhout (GEOPHYSICS, 2006). *The Cyclic Nature of Innovation: Connecting Hard Sciences with Soft Values* by Berkhout et al. (Elsevier JAI Press, 2007). “Coding and decoding: Seismic data modelling, acquisition and processing” by Ikelle, (SEG 2007 *Expanded Abstracts*). *Controlled illumination in prestack seismic migration*, By Rietveld (PhD thesis, 1985). “Acquisition using simultaneous sources” by Stefani et al. (EAGE 2007 *Extended Abstracts*, 2007). “Simplan: Simulated plane wave exploration” by Taner (SEG 1976 *Expanded Abstracts*). “Estimation of multiple scattering by iterative inversion, Part II: Practical Aspects and examples” by Verschuur and Berkhout (GEOPHYSICS, 1997). **TLE.**

Acknowledgements. Thanks to Eric Verschuur, Gerrit Blacquière, and Jan Thorbecke for their contribution to the illustrations and examples. Thanks also to the Delphi sponsors for the inspiring discussions on the impact of blending in the seismic industry.

Corresponding author: birchwood@hetnet.nl